Z. Angew. Math. Phys. 66 (2015), 1835–1851

0044-2275/15/041835-17
published online December 14, 2014
DOI 10.1007/s00033-014-0479-5

Zeitschrift für angewandte Mathematik und Physik ZAMP

Effective thermal conductivity of helium II: from Landau to Gorter–Mellink regimes

M. Sciacca, D. Jou and M. S. Mongiovì

Abstract. The size-dependent and flux-dependent effective thermal conductivity of narrow channels filled with He II is analyzed. The classical Landau evaluation of the effective thermal conductivity of quiescent He II is extended to describe the transition to fully turbulent regime, where the heat flux is proportional to the cubic root of the temperature gradient (Gorter–Mellink regime). To do so, we use an expression for the quantum vortex line density L in terms of the heat flux considering the influence of the walls. From it, and taking into account the friction force of normal component against the vortices, we compute the effective thermal conductivity as a function of the heat flux, and we discuss in detail the corresponding size dependence.

Mathematics Subject Classification. 76A25 · 76F06 · 80A20.

Keywords. Thermal conductivity · Liquid helium · Quantum turbulence · Micropores · Quantized vortices.

1. Introduction

Heat transport in small systems or in systems with microscale parts is an active frontier in technology, transport theory, non-equilibrium thermodynamics and statistical mechanics. One of the paradigmatic situations is the analysis of heat transport along very thin and long wires or channels, whose radius is comparable to the mean free path of the heat carriers—as for instance in silicon nanowires with phonons as heat carriers. In this paper, we consider a narrow channel filled with He II and analyze its transport properties—namely its effective thermal conductivity—in terms of the heat flux and the radius.

The high thermal conductivity of superfluid liquid helium (He II) makes it an excellent coolant material, with an important number of applications as, for instance, the refrigeration of superconducting magnets in particle accelerators or space cryogenics [1–3]. The interest on the transport properties of He II in thin or very thin channels (for instance, diameter from 1 mm to 50 μm) was in fact an advanced forerunner of the later general interest in microfluidics [4–15]. Here, we study the effective thermal conductivity of cylindrical microchannels filled with He II, a topic of interest in refrigeration of small systems, in the behavior of porous systems, and in the research on the effects of the walls on the quantized vortex lines typical of superfluid turbulence, which is a topic of fundamental interest.

In the simplest computation of the effective thermal conductivity of He II, the resistance to the flow is assumed to be due to the viscosity of the normal component [16]. This leads to a heat flux which is proportional to the temperature gradient (Landau regime). However, when the heat flux is high enough, quantized vortices appear and form a vortex tangle which contributes to the overall resistance of the flow [17–23]. This implies a drastic reduction in the effective thermal conductivity, and a strong departure with respect to Fourier's law, since the heat flux becomes proportional to the cubic root of the temperature gradient (the so-called Gorter–Mellink regime). In the practice, this increase in thermal resistance may have dramatic consequences if, because of the sudden loss of cooling ability, the helium temperature crosses the lambda temperature (about 2.17 K), and the helium is no longer a superfluid but a normal fluid. Thus, a detailed analysis from Landau regime to Gorter–Mellink regime is relevant on practical grounds.

Here, instead of fully developed turbulence, a well-known topic in helium cryogenics, we focus our interest on the transition regime from laminar or Landau regime to turbulent or Gorter–Mellink regime. This is a topic of practical and theoretical interest, since an exact mathematical description of it is not given often, and the physical understanding is not yet sufficiently developed, even though an attempt was given by Arp in Ref. [7]. For instance, one of the aspects that are not yet well known is the influence of the walls on the quantized vortex tangle of turbulent superfluid, a topic which is especially relevant in narrow channels. This is the aim of our paper.

In particular, we are interested in analyzing an expression for an effective thermal conductivity $K_{eff}(T, R, L, \dot{Q})$ in terms of the radius R of the cylinder, the temperature T, the vortex line density L, and the heat current $\dot{Q}$. The first arguments on the thermal conductivity of He II raised in the half of the previous century [24–31]. In 1956, Mendelsohn reviewed the main experimental peculiarities of He II [31], and in particular the heat conductivity in channels for zero mass flow (he also dealt with nonzero mass flow, but here we are interested on the former one). As pointed out by Mendelsohn, heat conductivity does not follow the classical behavior, and it seemed to depend on the applied heat flux. It was discovered later that this dependence and the strange behavior of He II is addressed to the presence of vortex line density. But, at that time, the quantized vortex lines were unknown, and it was observed that the ratio between the gradient of temperature and the heat current, $\Delta T/\dot{Q}$, was not longer constant for an applied heat flux higher than a critical value, and that it was proportional to the second power of the heat current $\dot{Q}$. Mendelsohn [31] proposed a theoretical expression for $\Delta T/\dot{Q}$ which comes from the formula of the mutual friction force when inserted in the London's formula, which describes the laminar and the full turbulent regimes, but it is not so accurate nor physically clear in the transition between both regimes. These arguments were handled by many authors some years later. In particular, in 1970, Arp studied the laminar case and he tried to establish the rules according to which the transition from the laminar case to the turbulent cases occurs [7]. According to Arp, the first transition occurs when the superfluid velocity is higher than $v_{sc} = (\kappa/d)\ln(d/(2a))$, namely the critical velocity for the appearance of the first vortex, whereas the second transition occurs when the normal component becomes turbulent, and for this reason, he related TII turbulence to the critical value of the classical Reynolds number.

The aim of the current paper is to analyze the relation between ΔT and $\dot{Q}$ in terms of the vortex line density L in the transition between laminar and fully turbulent regimes, which are established in terms of the quantum Reynolds number [32]. The results will be obtained in terms of the one-fluid model (with internal variables) of extended thermodynamics [33] as well as in the two-fluid model [16,18,19]. This topic has been considered from the experimental point of view (see, for instance, [6,22,23]), but here we relate it to a theoretical model on the variation between L and $\dot{Q}$ in narrow channels, by means of a generalized Vinen's equation. In this way, we show the practical usefulness of a better theoretical understanding of the behavior of quantized vortices in narrow channels and in the complex transition regions from laminar to fully turbulent regime. We go further than some previous papers using a generalized Vinen's equation [22,23], because we are able to describe both the laminar-TI turbulent transition region, as the TI-TII turbulent transition region and the TII fully developed region. However, in contrast to Ref [23], we do not consider the metastable region between the laminar regime and the turbulent regime shown in the Tough's experiments [22,23], for which a more general equation for L has to be considered (see review [34]) and which is more difficult to observe than the regimes considered here.

In Sect. 2, we deal with the laminar situation, and we compare it with Landau and Tisza [16,35] two-fluid model for the evaluation of the effective thermal conductivity of He II in a cylindrical channel and evaluate such conductivity in the presence of quantum turbulence, taking into account the vortex resistance, which for fully developed turbulence corresponds to Gorter–Mellink regime. Section 3 is the original part of this paper: Starting from an evolution equation for the vortex line density incorporating the effects of the walls, we propose a mathematical description of the transition regime. Section 4 is devoted to conclusions and remarks.

2. Effective thermal conductivity of He II in cylindrical channels

In this section, we deal with the effective thermal conductivity of He II along a cylindrical duct. We describe heat transport in terms of the one-fluid model of extended thermodynamics [33] as well as the Landau-Tisza two-fluid model [16,35]. The basic results of this section are already known, but it is convenient to recall them to make this paper sufficiently self-contained and understandable for a general reader.

If He II is globally at rest, the motion of the normal component is compensated by an opposite flow of the superfluid component, in such a way that the net velocity of the total system vanishes, i.e., there is no net mass flow. This requires that at any time t, $\rho_s \bar{v}_s + \rho_n \bar{v}_n = 0$, where $\bar{v}_s$ and $\bar{v}_n$ are the average velocities of the superfluid and normal component on the transversal section of the tube, and ρ_s and ρ_n are the corresponding densities. This situation is called *counterflow* in literature on He II [18,21], and the relevant quantity here is the so-called counterflow velocity v_{ns}, given by

$$v_{ns} = \bar{v}_n - \bar{v}_s = \frac{\rho}{\rho_s}\bar{v}_n. \tag{2.1}$$

The second equality of the former equation directly follows from the mentioned condition of vanishing mass flow, namely $\rho_n \bar{v}_n + \rho_s \bar{v}_s = 0$. Note for further use that the heat flow is given by $\bar{q} = \rho S T \bar{v}_n = \rho_s S T v_{ns}$, with S the entropy per unit mass.

According to the one-fluid model with the heat flux $\mathbf{q}$ as internal variable [33,36], in stationary situation, neglecting the nonlinear terms in the derivatives of the fields variables, the dynamical equations are

$$\nabla \cdot \mathbf{v} = 0, \tag{2.2}$$

$$\nabla \cdot \mathbf{q} = 0, \tag{2.3}$$

$$\nabla p - \eta \nabla^2 \mathbf{v} + \beta T \eta \nabla^2 \mathbf{q} = 0, \tag{2.4}$$

$$\lambda_1 \nabla T + \beta T^2 \eta \lambda_1 \nabla^2 \mathbf{v} - \beta^2 T^3 \eta \lambda_1 \nabla^2 \mathbf{q} = \sigma^q, \tag{2.5}$$

where β is a coefficient which can be related to the moments of fluctuations, σ^q is the production term of the heat flux, p is pressure, η is the shear viscosity, and λ_1 can be interpreted as the heat conductivity.

The last two equations can be also written

$$\nabla p - \eta \nabla^2 (\mathbf{v} - \beta T \mathbf{q}) = 0, \tag{2.6}$$

$$\nabla p + \frac{1}{\beta T^2} \nabla T = \frac{1}{\beta T^2 \lambda_1} \sigma^q, \tag{2.7}$$

where the production term in absence of vortices can be chosen $\sigma^q = -\mathbf{q}$ [33], while a more general assumption is required to take into account of the presence of vortices.

2.1. Laminar situation: Landau regime

In this subsection, we assume that $\sigma^q = -\mathbf{q}$ while a more general assumption which takes into account of the presence of vortices will be the argument of the next subsection. Thus,

$$\nabla p - \eta \nabla^2 (\mathbf{v} - \beta T \mathbf{q}) = 0, \tag{2.8}$$

$$\nabla T + \beta T^2 \nabla p = -\frac{1}{\lambda_1} \mathbf{q}. \tag{2.9}$$

Thermal conductivity λ_1 is linked to the velocity of second sound w_2 by the relation $\zeta = \lambda_1/\tau_1 = w_2^2 \rho c_V$, where c_V is the constant volume specific heat and τ_1 the relaxation time of the heat flux [33] (the expression of ζ in terms of the parameters of the two-fluid model is given below Eq. (2.15)). It is experimentally observed that λ_1 is very high so that the right-hand side of the second equation in (2.9)

may be taken as zero. When (2.9) is applied to a cylindrical pipe filled with He II, it follows that the (2.8) is integrable along the pipe with a constant applied ∇p. In what follows, we assume that both the pressure gradient ∇p and temperature gradient ∇T do not depend on the spatial coordinate, and that $\mathbf{q}$ and $\mathbf{v}$ depends only on the local radius r. Then we find

$$v(r) - \beta T q(r) = \frac{\Delta p R^2}{4 l \eta} \left[1 - \frac{r^2}{R^2}\right], \tag{2.10}$$

where R and l are the radius and the length of the pipe, and the heat flux and velocity along the wall have been assumed to be zero (non-slip condition). Taking into account (2.9), with vanishing right-hand side, namely $\Delta p = -(\beta T^2)^{-1} \Delta T$, Δp and ΔT, respectively, being the pressure difference and the temperature difference between the longitudinal ends of the channels, the mean value of the heat flux over the transversal section of the pipe obtained from (2.10) may be expressed in terms of ΔT as

$$\bar{v} - \beta T \bar{q} = \frac{\Delta p R^2}{8 l \eta} = -\frac{\Delta T R^2}{8 l \beta T^2 \eta}. \tag{2.11}$$

According to the counterflow condition $\bar{v} = 0$, we obtain

$$\bar{q} = -\frac{\Delta p R^2}{8 l \beta T \eta} = \frac{\Delta T R^2}{8 l \beta^2 T^3 \eta}. \tag{2.12}$$

Therefore, since the total heat flux across the transversal area is $\dot{Q} = \pi R^2 \bar{q}$, the effective heat conductivity according to the Fourier's law is

$$K_{eff} = \frac{\dot{Q}}{\pi R^2} \frac{l}{\Delta T} = \frac{R^2}{8 \beta^2 T^3 \eta} = \frac{R^2 \rho^2 T S^2}{8 \eta}. \tag{2.13}$$

We have used $\beta = -(\rho S T^2)^{-1}$ [33] to make evident that (2.13) is the well-known Landau formula for thermal conductivity [1,16,36,37]. Note that (2.13) is not a true thermal conductivity, dependent only on the material, but a global quantity, that depends quadratically on the radius R of the cylinder, and therefore, it is strongly reduced for thin capillaries.

2.2. Turbulent situation: Gorter–Mellink regime

Let's now take into account the presence of quantum vortices in He II, when the heat flux becomes higher than a threshold value. The presence of the vortices is described by the vortex length density L, and their main effect on the flow is an internal friction between the vortices and the normal fluid [17–21].

In the one-fluid model [33,36,38], the effects of the internal friction are described through a contribution to the production term σ^q appearing in Eq. (2.7), which is taken now as $\sigma^q = -\mathbf{q} - \tau_1 K L \mathbf{q}$, where $K = \frac{1}{3}\kappa B_{HV}$, B_{HV} being the dimensionless Hall-Vinen friction coefficient, κ the quantum of circulation h/m (with m the mass of helium atom and h the Planck's constant in such a way that $\kappa = 9.97 \times 10^{-8} \mathrm{m}^2/\mathrm{s}$), and τ_1 the relaxation time of the heat flux. Hence, Eqs. (2.8) and (2.9) become

$$\nabla p - \eta \nabla^2 (\mathbf{v} - \beta T \mathbf{q}) = 0, \tag{2.14}$$

$$\nabla T + \beta T^2 \nabla p = -\frac{1}{\lambda_1} \mathbf{q} - \frac{KL}{\zeta} \mathbf{q}, \tag{2.15}$$

where $\zeta = \lambda_1/\tau_1$ as said below Eq. (2.9), and which in the two-fluid theory is $\zeta = \lambda_1/\tau_1 = \frac{\rho T S^2 \rho_s}{\rho_n}$. Assuming that λ_1 is very high to neglect the first term in the right-hand side of (2.15), but comparable

to the relaxation time τ_1 in such a way that ζ is finite (it also determines the second sound velocity as said below (2.9)), Eqs. (2.14) and (2.15) reduce to

$$\nabla p - \eta\nabla^2(\mathbf{v} - \beta T\mathbf{q}) = 0, \tag{2.16}$$

$$\nabla T + \beta T^2\nabla p + \frac{KL}{\zeta}\mathbf{q} = 0. \tag{2.17}$$

The solution of (2.16) applied to He II in a cylindrical pipe is still (2.10), and the mean value is (2.12). By integrating the second equation of (2.17) along the pipe, we find

$$\Delta T + \beta T^2\Delta p = \frac{Kl\bar{L}}{\zeta}\bar{q}, \tag{2.18}$$

where $\nabla T = -\Delta T/l$, $\nabla p = -\Delta p/l$ and $\bar{L}$ is the mean value of the vortex line density. In Ref. [39] the authors studied the stability of the normal component (which is proportional to the heat flux $\mathbf{q}$) proving that the Poiseuille flow is stable when the vortex line density L is assumed to be constant inside the channel. We do not consider in detail any dependence of L on the distance r from the wall of the channel but only the mean value. In what follows, L stands for $\bar{L}$. Then, by using (2.16), in view of the previous identification of β as $\beta = -(\rho S T^2)^{-1}$, and writing Δp in terms of $\bar{q}$ one obtains

$$\Delta T = \frac{8\eta l}{R^2\rho^2 S^2 T}\bar{q} + \frac{KlL}{\zeta}\bar{q}. \tag{2.19}$$

From here, it follows that the effective thermal conductivity is

$$K_{eff} = \frac{R^2\zeta}{8\beta^2 T^3\eta\zeta + KLR^2}. \tag{2.20}$$

Equation (2.19) may also be written in terms of $\dot{Q}$ as

$$\Delta T = \frac{8\eta l}{\pi R^4\rho^2 S^2 T}\dot{Q} + \frac{KlL}{\pi R^2\zeta}\dot{Q}. \tag{2.21}$$

The first term corresponds to Landau regime; if one takes $L \sim \dot{Q}^2$, the second term corresponds to the Gorter–Mellink regime. We want to study the transition from one to the other.

3. Transition from Landau to Gorter–Mellink regime

Our aim is to propose a mathematical description for the transition from Landau to Gorter–Mellink regimes. Thus, instead of directly taking $L \propto \dot{Q}^2$ in (2.21), which is typical of fully developed turbulence in wide channels, we pay attention to a more detailed relation between L and $\dot{Q}$ in narrow channels in steady state situations.

In fact, the mentioned transition implies a narrow intermediate regime (TI turbulence) [18–21], with a relatively low vortex line density and a transition to a more developed turbulence (TII turbulence). According to experimental results [22], a relevant quantity in such transition is the quantum Reynolds number $v_{ns}d/\kappa$, with v_{ns} the counterflow velocity, d the diameter of the channel and κ the quantum of circulation. Since κ has dimensions of (length)^2/time it plays in $v_{ns}d/\kappa$ a role analogous to that of kinematical viscosity ν in classical Reynolds number Vd/ν, with V the velocity [32]. In Ref. [7], Arp instead considers the classical Reynolds number $\rho v_n d/\eta$ (ρ, η and v_n being the density and viscosity of He II and the velocity of the normal component, respectively, and d the diameter of the channel), because he assumes that TII turbulence is caused by the turbulence of the normal component.

For instance, in wide channels, the transition from laminar regime to the first kind of turbulence (TI turbulence) is at quantum Reynolds number $Re_1 = 127$ at $T = 1.5$ K (for $\dot{Q} = 5\times10^{-4}$ J/s the diameter for which this transition will be detected is $d = 1{,}330\,\mu$m, and for $\dot{Q} = 10\times10^{-4}$ J/s, $d = 2{,}650\,\mu$m) [32]. A further transition to TII turbulence is found at quantum Reynolds number $Re_2 = 226$, which

yields the values $d = 740\,\mu\text{m}$ (for $\dot{Q} = 5 \times 10^{-4}$ J/s) and $d = 1{,}490\,\mu\text{m}$ (for $\dot{Q} = 10 \times 10^{-4}$ J/s). At $T = 1.6$ K, the respective values of the mentioned critical quantum Reynolds numbers are $Re_1 = 112$ and $Re_2 = 212$, and at $T = 1.7$ K they are $Re_1 = 96$ and $Re_2 = 187$. Note the dependence of these values on the temperature. All these complexities must be taken into account in order to describe the transition from Landau to Gorter–Mellinck regime, as we do below.

3.1. Relation between vortex length density and heat flux q in narrow channels

In order to take into account the presence of the vortex lines, the model proposed in the previous sections needs to be completed by adding an evolution equation for the vortex line density L. It usually refers to the classical Vinen's equation for the evolution of L [17–21]

$$\frac{\mathrm{d}L}{\mathrm{d}t} = \alpha_v v_{ns} L^{3/2} - \beta_v \kappa L^2, \tag{3.1}$$

with α_v and β_v dimensionless coefficients which depend on T and which are related to vortex formation and destruction, respectively. The steady-state result of (3.1) is

$$L^{1/2} = \frac{\alpha_v}{\beta_v \kappa} v_{ns} = \frac{\alpha_v}{\beta_v \kappa \rho_s T S} \bar{q}, \tag{3.2}$$

leading to $L \propto q^2$. This corresponds to fully developed turbulence. However, Eq. (3.1) and its stationary solution do not take into account the presence of the wall, and the stationary solution does not describe the transition from the TI turbulent regime to the TII turbulent regime obtained experimentally by Martin and Tough [22]. For this reason, such a transition may be described by means of a generalized Vinen's equation including the wall effects, which, in the simplest version is [34,38]

$$\frac{\mathrm{d}L}{\mathrm{d}t} = -\beta_v \kappa L^2 + \left[\alpha_0 v_{ns} - \omega' \beta_v \frac{\kappa}{d}\right] L^{3/2}, \tag{3.3}$$

with d the diameter of the tube, and the coefficients α_0 and ω are functions of $v_{ns}d/\kappa$, the quantum Reynolds number and of the temperature T. The third term takes into account the effect of having a thin tube with diameter d finite, and therefore, it modelizes the influence of the wall. For narrow channels, this term—absent from (3.1)—becomes especially relevant, whereas it becomes negligible for wide channels. For the aims of the present paper, we are interested in the steady state of the differential equation (3.3), as made in the previous section, which means to assume a constant value for the vortex line density L in the channel. This has been observed experimentally and numerically, for example, in [22,40].

Equation (3.3) has the steady-state solutions

$$L = 0; \qquad L^{1/2} = \frac{\alpha_0}{\beta_v \kappa} v_{ns} - \frac{\omega'}{d}. \tag{3.4}$$

The nonzero solution exists and is stable for $v_{ns} > V_{c1} = \frac{\beta_v \kappa \omega'}{\alpha_0 d}$. From the experimental results reported in [22], it is seen that the second kind of solution has two different regimes, namely a TI turbulence for a quantum Reynolds number $Re = v_{ns}d/\kappa$, between Re_1 and Re_2 , described by [22]

$$L^{1/2} = \frac{\gamma_{TI}}{\kappa} v_{ns} - 1.48 \frac{\alpha_1}{d}, \tag{3.5}$$

and TII turbulence flow for $Re > Re_2$ described by [22]

$$L^{1/2} = \frac{\gamma_{TII}}{\kappa} v_{ns} - 1.48 \frac{\alpha_2}{d}, \tag{3.6}$$

with γ_{TI}, γ_{TII} and α_i numerical constants which depend on temperature. The parameter γ_{TI} does not depend on the diameter of the channel as concluded by Martin and Tough's paper [22]. The parameter α_1 instead is a weakly increasing function of the diameter d and the conclusion of Tough's group is that $\alpha_1 \simeq 5$ for wide channels (about $d = 10^{-3}$ m) and $\alpha_1 \simeq 1$ for narrow channels (about $d = 1.2 \times 10^{-4}$

m), and for smaller diameters we obtain it should be smaller (in Fig. 6 our model fits well the data for $\alpha_1 = -1$ for $d = 61\,\mu$m). For the parameters γ_{TII} and α_2, we do not have enough information from the experiments and we assume they depend on T and d as γ_{TI} and α_1. In Table 1, we report γ_{TI} and α_1 taken from Table I in Ref. [22], whereas γ_{TII} and α_2 are obtained by fitting the experimental data from Figure 10 in Ref. [22]. The second solution in (3.4) fits the experimental data [22] in the TI regime for $\frac{\alpha_0}{\beta_v} = \gamma_{TI}$ and $\omega' = 1.48\alpha_1$, whereas in the TII regime for $\frac{\alpha_0}{\beta_v} = \gamma_{TII}$ and $\omega' = 1.48\alpha_2$.

The transition from the TI turbulent regime to the TII turbulent regime can be described in (3.3) by assuming that coefficient α_0 depends on the quantum Reynolds number Re as [38]

$$\gamma_0(Re) = \frac{\alpha_0(Re)}{\beta_v} = \alpha_c\,(1 + c\tanh\left[A\,(Re - Re_2)\right]) \tag{3.7}$$

in such a way that $\gamma_0(Re) = \gamma_{TI}$ for $Re_1 \ll Re \ll Re_2$ and $\gamma_0(Re) = \gamma_{TII}$ for $Re \gg Re_2$, with $\alpha_c = \frac{\gamma_{TI}+\gamma_{TII}}{2}$ and $c = \frac{\gamma_{TII}-\gamma_{TI}}{\gamma_{TI}+\gamma_{TII}}$. The coefficient A is chosen to fit better the transition regime from turbulence TI and turbulence TII. In figures below, we have chosen $A = 1.47/(Re_{\rm edge} - Re_2)$, where $Re_{\rm edge} = V_{\rm edge}d/\kappa$ with $V_{\rm edge}$ being the counterflow velocity which guarantees the 90 % of the codomain of tanh between the edges of the transition interval. In Table 1 we report the difference $V_{\rm edge} - V_{c2}$ from Ref [22], which is the gap of the counterflow velocity in the transition region between TI and TII turbulent regimes (see figures below). We use the same value both for wide and narrow channels.

Also, an expression similar to (3.7) is required for the coefficient ω' [38]

$$\omega'(Re) = \beta_c\,(1 + c_1\tanh\left[A\,(Re - Re_2)\right]) \tag{3.8}$$

with $\beta_c = 0.74(\alpha_1 + \alpha_2)$ and $c_1 = \frac{\alpha_2-\alpha_1}{\alpha_1+\alpha_2}$, in such a way $\omega' = 1.48\alpha_1$ in the TI regime and $\omega' = 1.48\alpha_2$ in the TII regime.

In Fig. 1 the second solution (3.4) with (3.7) and (3.8) (the blue line) is compared with the experimental results by Martin and Tough [22] (dots) for the TI regime (3.5) (the yellow line) and for the TII regime

TABLE 1. *In the table temperature T (K), helium density ρ (Kg m^{-3}), dynamic viscosity η (Kg (s m)$^{-1}$), density of the superfluid component ρ_s (Kg m^{-3}), specific entropy S (J (Kg K)$^{-1}$) and dimensionless parameters B_{HV} are from [41]*

T	ρ	η	ρ_s	γ_{TI}	B_{HV}	S	$V_{\rm edge} - V_{c2}$
1.5	145	1.35×10^{-6}	129	7.68×10^{-2}	1.296	196	1.7×10^{-3}
1.6	145	1.3×10^{-6}	122	8.57×10^{-2}	1.193	282	1.2×10^{-3}
1.7	145	1.29×10^{-6}	112	9.17×10^{-2}	1.1	395	0.7×10^{-3}

Parameter γ_{TI} is taken from Table I in Ref. [22]. The values reported here depend only on temperature and they are used for all the figures of this paper

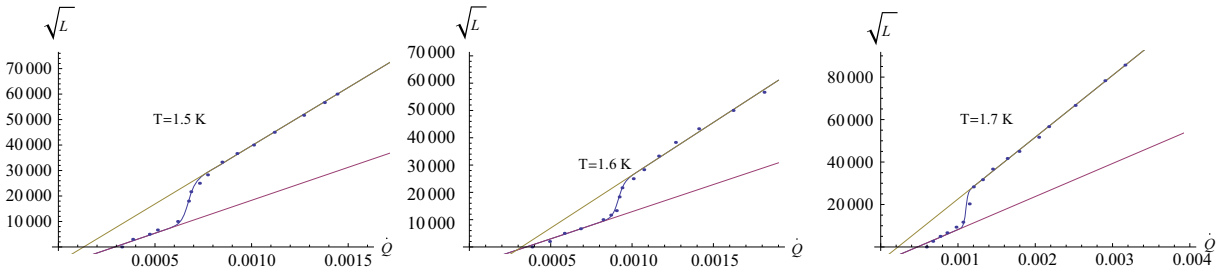

FIG. 1. [Color online] Plot of $L^{1/2}$ (m^{-1}) versus the heat flux $\dot{Q}$ (J/s) for three temperatures $T = 1.5$ K (*left*), $T = 1.6$ K (*middle*) and $T = 1.7$ K (*right*). In each figure the two regimes TI (*the lower one*, or bordeaux) and TII (*the upper one*, or *yellow*), given by the *straight lines* are compared with our solution (3.4b) with γ_0 and ω' given in (3.7) and (3.8) and for $d = 10^{-3}$ m. The *experimental dots* correspond to the results in Ref. [22]

(3.6) (the bordeaux line). Plots refer to three different temperatures: $T = 1.5$ K (the left figure), $T = 1.6$ K (the middle figure) and $T = 1.7$ K (the right figure).

In the next section, we directly go to the experimental results obtained by Tough and collaborators on heat transfer in He II in cylindrical channels [22]. For high v_{ns}, Eq. (3.6) may be approximated by $L^{1/2} = \gamma_{TII} v_{ns}$, and (2.21) becomes analogous to the Mendelsohn's proposal, but for intermediate values of v_{ns} corresponding to $Re_1 < Re < Re_2$ and slightly above Re_2, Eqs. (3.5) and (3.6), or (3.4b) must be used.

The physical model underlying the modelization (3.7) and (3.8), is the assumption of a sudden increase of the vortex length density in the transition TI–TII, but with laminar behavior of the normal component. This is in contrast with Arp's assumption that turbulence TII is due to turbulence of the normal component. The mentioned increase in L is interpreted as the reconnection of Kelvin waves along pinned vortex lines of TI turbulence. Such a reconnection produces a high number of free vortex loops whose length increases with increasing heat flux in a steeper way than for TI turbulence. In fact, the discussion about the physical nature of turbulence TII is still an open topic, as well as the transition from TI to TII.

3.2. Quantum turbulence: explicit evaluation

In the previous sub-section, we have seen that thermal conductivity depends on the vortex line density, which in wide channels is related to the counterflow velocity in a very direct and simple way. However, in narrow channels, L depends also on the diameter of the channel, as shown by Tough and collaborators in their studies over the 1980's [22,23]. This happens when radius becomes comparable to the average separation of vortex lines, which is of the order of $L^{-1/2}$. They obtained that He II is laminar without vortex lines, for $Re < Re_1$ (except some remaining vortex lines of previous experiments, pinned to the walls or formed at the λ-transition); for $Re_1 < Re < Re_2$ there is the so-called turbulence TI: a mild form of turbulence characterized by a relatively low value of L (3.5); for $Re > Re_2$ there is a steep increase in L, and the value of L (3.6) increases for increasing Re. The values of the critical Reynolds numbers depend on the temperature as well as on the diameter d of the channel and they are reported in Table 3.

In Ref. [32], we have defined the quantum Reynolds number $Re = \dfrac{v_{ns} d}{\kappa}$. Now, using (3.5) we can write the quantum Reynolds number in terms of L as

$$Re = \frac{v_{ns} d}{\kappa} = \frac{L^{1/2} d + 1.48 \alpha_1}{\gamma_{TI}}. \tag{3.9}$$

Martin and Tough found that in the turbulent TI regime one has $L^{1/2} d \simeq 2.5$ both in wide channels and in narrow channels [22]. Note that, the independence of $L^{1/2} d$ and γ_{TI} on the diameter of the channel shows that in the TI regime $Re(d)$ only depends on the channel size for the mild dependence of the parameter α_1 on d, which we have commented above. In Table 3, we report the values of the Reynolds number both for wide channels and for narrow channels at three different temperatures: The values of Re for wide channels are taken from the experiments in Ref. [22] (and they satisfy approximately well formula (3.9)), whereas the values for the narrow channels are obtained using formula (3.9) and $\alpha_1 = 1$.

The second transition from TI to TII turbulent regimes occurs for Re_2 which still satisfy formula (3.9) but for $L^{1/2} d \simeq 10$ as obtained by the Tough's group [22] [see their formula (19) and the corresponding Figure 12].

It's worth to note that the second transition from TI to TII turbulent regime in experiments shown in Figure 11 of Ref. [23] at $T = 1.6$ K (reported in our Fig. 5) does not satisfy $Re_2 = 134$, but $Re_2 = 101$ (which is the value used to fit the data in Fig. 5).

The explanation of this steep increase of L is still open to debate because there isn't a definitive proof, even experimentally, of what these two states, TI and TII, are. But, it is worth mentioning two

different possible explanations: the one proposed by two of us in Ref. [38] and the one proposed by Melotte and Barenghi in Ref. [7,42]. The former interpreted the steep increase of L at Re_2 as the beginning of vortex reconnection, namely, to the production of a high number of free vortex loops as a consequence of the crossing and cutting and recombining of vortex lines that in turbulence TI were most of them pinned to the walls [43]. The increase of L in turbulence TI, instead, is basically due to Kelvin wave excitations in pinned vortex lines. The second proposal, instead, of Melotte and Barenghi [42] explains this transition to the TII state as a consequence of the transition from laminar to turbulence flow for the normal component. However, the critical velocity for superfluid turbulence is of one order smaller than the critical velocity for the normal component. Of course, each proposal does not preclude the other one, and a combined interplay of the two proposals is also possible.

The description of ΔT in terms of $\dot{Q}$ will be

$$\Delta T = \frac{8\eta l}{\pi R^4 \rho^2 S^2 T}\dot{Q} \qquad \text{for} \qquad Re < Re_1; \tag{3.10}$$

$$\Delta T = \frac{8\eta l}{\pi R^4 \rho^2 S^2 T}\dot{Q} + \frac{Kl}{\zeta}\left[\frac{\gamma_0}{\kappa \rho_s T S}\frac{\dot{Q}}{\pi R^2} - \frac{\omega'}{2R}\right]^2 \frac{\dot{Q}}{\pi R^2}, \qquad \text{for} \qquad Re > Re_1; \tag{3.11}$$

where

$$\gamma_0 = \frac{\gamma_{TI} + \gamma_{TII}}{2}\left(1 + \frac{\gamma_{TII} - \gamma_{TI}}{\gamma_{TII} + \gamma_{TI}} \tanh\left[A\left(Re - Re_2\right)\right]\right) \tag{3.12}$$

$$\omega' = 0.74(\alpha_1 + \alpha_2)\left(1 + \frac{\alpha_2 - \alpha_1}{\alpha_1 + \alpha_2} \tanh\left[A\left(Re - Re_2\right)\right]\right) \tag{3.13}$$

where Re can be expressed in terms of $\dot{Q}$ by $Re = \frac{2v_{ns}R}{\kappa} = \frac{2\dot{Q}}{\kappa\rho_s TS\pi R}$ and $A = \dfrac{1.47\kappa}{d(V_{\text{edge}} - V_{c2})}$ can be evaluated assuming that the 90 % of the codomain of tanh is between the edges of the transition interval (the values are shown in Table 1 and are taken from the Martin and Tough's experiments in wide channels

TABLE 2. *In this table we report the different values of α_1, γ_{TII} and α_2 used in our figures for different T and d*

T	d	α_1	γ_{TII}	α_2
Wide channels				
1.5	1,000 μm	5.1	13.57×10^{-2}	4.04
1.6	1,000 μm	4.7	16.67×10^{-2}	8.38
1.7	1,000 μm	5	17.14×10^{-2}	4.4
Narrow channels				
1.6	126 μm	1	8.8×10^{-2}	0
1.6	61 μm	−1	8.8×10^{-2}	−2
1.7	50 μm	−1	10×10^{-2}	−2

Wide channels refer to d of the order 1,000 μm or higher, and narrow channels to d of the order of 100 μm or smaller

TABLE 3. *In the table the critical quantum Reynolds numbers Re_1 for the appearance of TI turbulent regime and Re_2 for the appearance of TII turbulent regime for three temperatures are reported both in wide and narrow channels from the Martin and Tough's experiments [22] and formula* (3.9)

T	1.5 K	1.6 K	1.7 K
Wide channels			
Re_1	127	112	96
Re_2	226	212	187
Narrow channels			
Re_1	52	46	43
Re_2	149	134	125

Wide channels refer to d of the order 1,000 μm or higher, and narrow channels to d of the order of 100 μm or smaller

but used also for narrow channels). From the second term in the rhs of Eq. (3.11), one obtains the critical value $\dot{Q}_c = \frac{\omega' \kappa \rho_s T S \pi R}{2\gamma_0}$. In all the figures plotted in this paper, we use the values of Table 1 for both narrow and wide channels, and the values in Tables 2 and 3 for, respectively, wide and narrow channels.

These expressions for the vortex line density in narrow channels allow to obtain the effective thermal conductivity, which now depends not only on the radius but also on the applied heat current $\dot{Q}$

$$K_{\text{eff-turb}} = \frac{T\rho^2 S^2 R^2 \zeta}{8\eta\zeta + KT\rho^2 S^2 R^2 \left(\frac{\gamma_0}{\kappa\rho_s TS}\frac{\dot{Q}}{\pi R^2} - \frac{\omega'}{2R}\right)^2}, \tag{3.14}$$

where the relation $\dot{Q} = \pi R^2 q = \pi R^2 \rho_s T S v_{ns}$ has been used, and consequently the ratio between $K_{\text{eff-Landau}}$ and $K_{\text{eff-turb}}$ becomes

$$\frac{K_{\text{eff-Landau}}}{K_{\text{eff-turb}}} = 1 + \frac{KR^2\rho^2 S^2 T}{8\eta\zeta}\left(\frac{\gamma_0}{\kappa\rho_s TS}\frac{\dot{Q}}{\pi R^2} - \frac{\omega'}{2R}\right)^2. \tag{3.15}$$

We apply our results (3.10)–(3.11) and (3.15) to the experiments of Martin and Tough [22], who made systematic measurements on heat transfer in He II in cylindrical channels. We take $d = 1{,}000\,\mu$m, $l = 10$ cm and $T = 1.5$ K, $T = 1.6$ K and $T = 1.7$ K. In Tables 1, 2 and 3, the values of the parameters used in the calculations are reported. Thermal conductivities (3.15) from the Martin and Tough's experiments are drawn in Fig. 2 for three different temperatures ($T = 1.5$ K, $T = 1.6$ K and $T = 1.7$ K) against the heat current $\dot{Q}$. For the same values, the ratio $\Delta T/\dot{Q}$ versus $\dot{Q}$ is plotted in Fig. 3 for (3.10)–(3.11) in order to compare it to the experimental data from [31].

The same expression (3.15) is then plotted in Fig. 4 at two fixed applied heat flux: $\dot{Q} = 5 \times 10^{-4}$ J/s and $\dot{Q} = 10 \times 10^{-4}$ J/s for $Re > Re_1$. For these plots, we used the values of the tables corresponding to wide channels, because we do not know the exact dependence of some coefficients (i.e., α_1) on the diameter d of the channel. It is worth to note that we plotted the ratio (3.15) also for the values of the coefficients in the tables corresponding to narrow channels and the behavior of the figures is only slightly different than that shown in Fig. 4, and for this reasons, we have avoided to report. Since we don't know the exact expression for α_1 in terms of the diameter d of the channels in (3.9) we write v_{ns} in terms of the

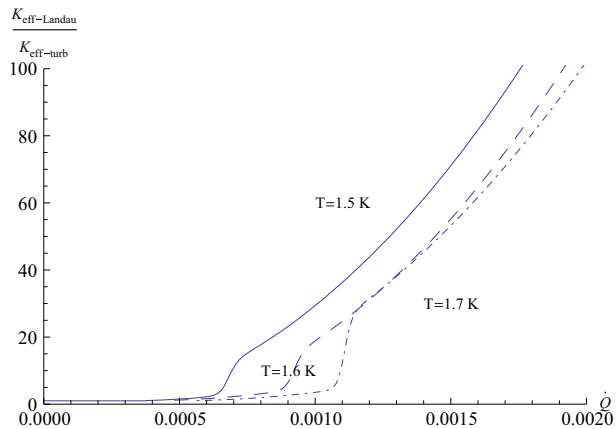

FIG. 2. The behaviour of the ratio between thermal conductivity in superfluid helium without and with vortices (3.15) against the applied heat current $\dot{Q}$ (J/s) in the Martin and Tough's experiment for diameter $d = 1{,}000\,\mu$m at three different temperatures, $T = 1.5$ K (*solid line*), $T = 1.6$ K (*dashed line*) and $T = 1.7$ K (*dot-dashed line*). The transition between the TI turbulence to TII turbulence is clearly visible in the elbow of the *plot*

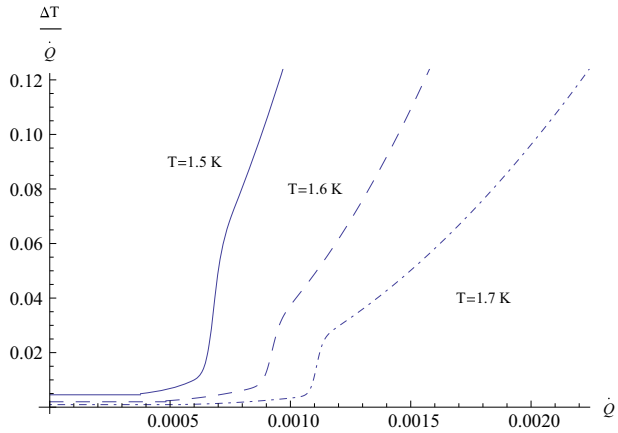

FIG. 3. Behaviour of the ratio $\Delta T/\dot{Q}$ (K s/J) versus $\dot{Q}$ (J/s) according to (3.11) in superfluid helium in the TI and TII regimes. Data are from the Martin and Tough's experiment for radius 1,000 μm at three different temperatures: $T = 1.5$ K (*solid line*), $T = 1.6$ K (*dashed line*) and $T = 1.7$ K (*dot-dashed line*)

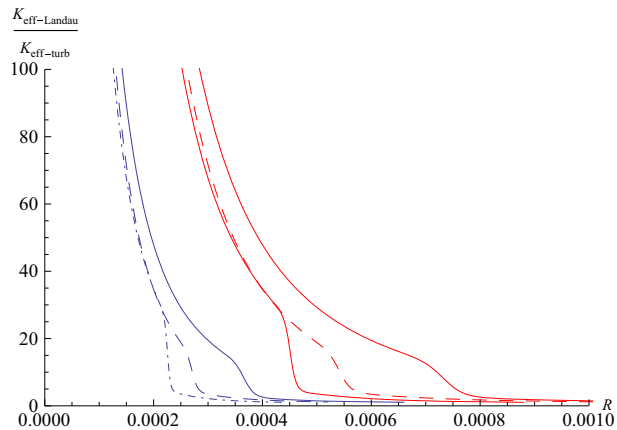

FIG. 4. Behaviour of the ratio between thermal conductivity in He II without and with vortices according to (3.15) against the radius of the channel (m). The *blue line* refers to an applied heat current $\dot{Q} = 5 \times 10^{-4}$ J/s whereas the *red lines* refers to an applied heat current $\dot{Q} = 10^{-3}$ J/s. Each case is considered for three temperatures: $T = 1.5$ K (*solid line*), $T = 1.6$ K (*dashed line*) and $T = 1.7$ K (*dot-dashed line*)

heat current $\dot{Q}$, namely $Re = \frac{2\dot{Q}}{\kappa\rho_s TS\pi R}$. Then, the turbulent status for an applied heat current in terms of the radius of the channel can be established. Indeed, from $\frac{2\dot{Q}}{\kappa\rho_s TS\pi R} > Re_1$, we find $R < \frac{2\dot{Q}}{\kappa\rho_s TS\pi Re_1}$, namely the narrower is the tube the higher is the turbulent vortex line density L. Figure 4 shows that in channels with small diameter the effective thermal conductivity is small and decreases with the diameter. Note that in Fig. 4, a cutoff in the radius of the channel has to be considered because for diameter small enough the quasiparticle of superfluid helium cannot flow through the narrow channel and a ballistic regime is reached, which will not be discussed here [6,44].

For the critical Reynolds number Re_1 considered in wide channels, the critical radius corresponding to the applied heat currents $\dot{Q} = 5 \times 10^{-4}$ J/s and $\dot{Q} = 10 \times 10^{-4}$ J/s are, respectively: $r_c = 660\,\mu$m

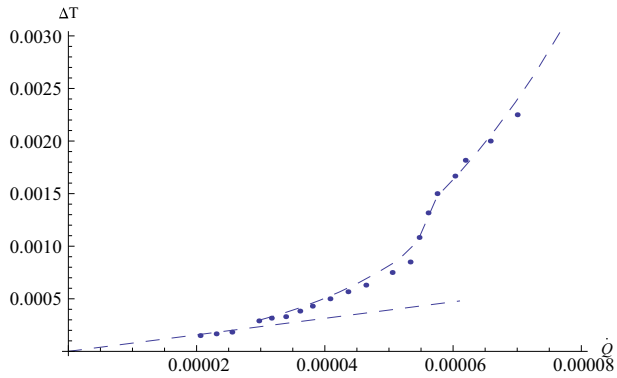

FIG. 5. The results of Eqs. (3.10) and (3.11) are plotted in order to reproduce the experimental data of Figure 11 in Ref. [23] for $d = 124\,\mu$m at $T = 1.6$ K. The values of the parameters used are reported in the Tables 1, 2 and 3 ($\gamma_{TI} = 8.57 \times 10^{-2}$, $\alpha_1 = 1$ is that proposed by Martin and Tough, and $\gamma_{TII} = 8.8 \times 10^{-2}$ and $\alpha_2 = 0$ are the values which better fit the experimental data)

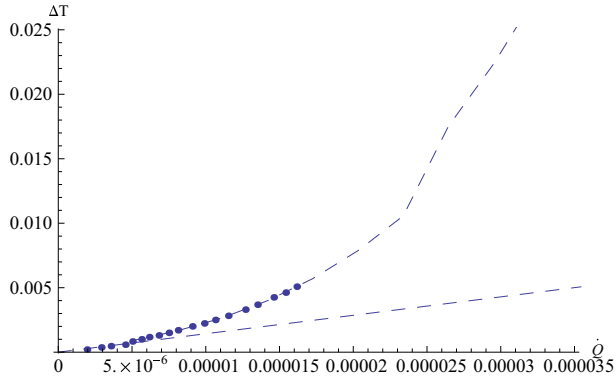

FIG. 6. The results of Eqs. (3.10) and (3.11) are plotted in order to reproduce the experimental data of Figure 14 in Ref. [23] for $d = 61\,\mu$m at $T = 1.6$ K. The values of the parameters used are reported in the Tables 1, 2 and 3 ($\gamma_{TI} = 8.57 \times 10^{-2}$, $\alpha_1 = -1$ is the best fit of the data, $\gamma_{TII} = 8.8 \times 10^{-2}$ and $\alpha_2 = -2$)

and $r_c = 1{,}330\,\mu$m (for $T = 1.5$ K); $r_c = 750\,\mu$m and $r_c = 1{,}500\,\mu$m (for $T = 1.6$ K); $r_c = 440\,\mu$m and $r_c = 880\,\mu$m (for $T = 1.7$ K).

In Figs. 6 and 7 of the Arp's paper, the author plots ΔT versus $\dot{Q}$ at two temperatures ($T = 1.5$ K and $T = 1.9$ K) for different diameters of the channel but in the laminar case. More precisely, the author estimates the two critical thermal heat flux for the appearance of the mutual friction effects due to the presence of quantized vortices. For Arp, the transition from the laminar case to the turbulent case is ruled in good approximation by the critical superfluid velocity $v_{sc} = (\kappa/d)\ln(d/(2a))$ with d the diameter of the channel and $a = 10^{-10}$ m the empirical vortex core. If we rewrite the critical Reynolds number $Re_1 = v_{ns}d/\kappa$ in terms of the critical velocity v_{sc} used by Arp we find $Re_1 = (\rho/\rho_n)v_{sc}d/\kappa = (\rho/\rho_n)\ln(d/(2a))$, which depends on the temperature by the ratio ρ/ρ_n. This expression for Re_1 is a possible theoretical choice, which would confirm our calculations (see second and third paragraphs of Sect. 3) in the decrease of Re_1 versus the temperature T.

In Fig. 5, we have reported the experimental data of Figure 11 of Ref.[23] at $T = 1.60$ K in a narrow channel of $d = 126\,\mu$m (dots) and Eq. (3.10) (straight line) and Eq. (3.11) (curve). Our equations fit quite well the experimental data. In these plots, the values of α_1 and γ_{TI} are those proposed by Tough's group with $\alpha_1 = 1$ in narrow channels and for γ_{TI} the same value adopted in wide channels (confirming the

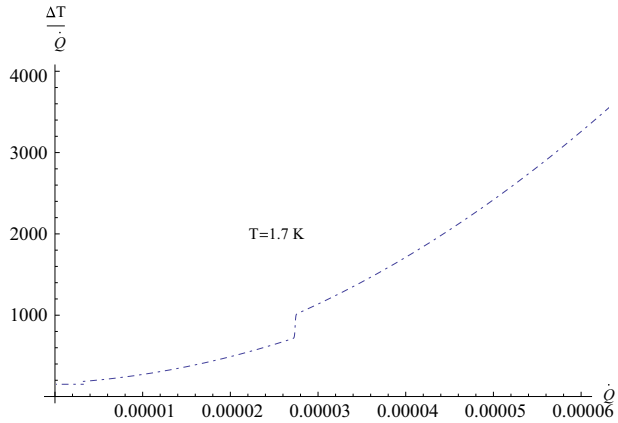

FIG. 7. Behaviour of the ratio $\Delta T/\dot{Q}$ (K s/J) versus $\dot{Q}$ (J/s) according to (3.11) in He II for a microchannel filled with helium II with diameter 50 μm at $T = 1.7$ K

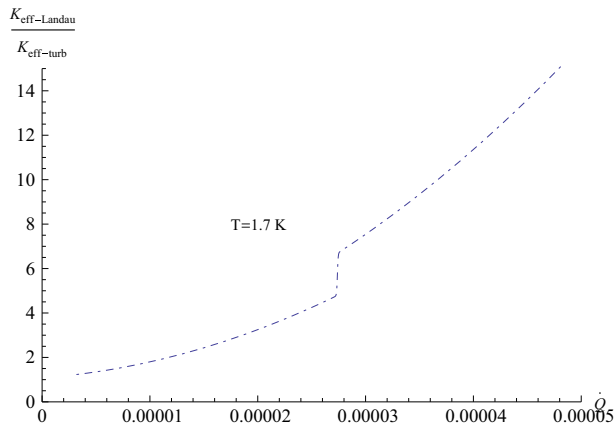

FIG. 8. The behaviour of the ratio between thermal conductivity in He II without and with vortices according to (3.15) against the applied heat current $\dot{Q}$ (J/s) in a micro channel with a diameter of 50 μm at $T = 1.7$ K. The transition between the TI turbulence to TII turbulence is clearly visible in the elbow of the *plot*

independence of the diameter d of the channel). The value of α_2 ($\alpha_2 = 0$) and γ_{TII} ($\gamma_{TI} = 8.8 \times 10^{-2}$) are chosen in order to fit the data. A further note is that the first transition satisfies formula (3.9), but not the second transition for which the value $Re_2 = 101$ has been obtained. The difference $V_{\text{edge}} - V_{c2}$ is kept equal to that in wide channels.

Then, we have taken into account the experimental data from Figure 14 of Ref. [23] at $T = 1.6$ K for a narrower channel $d = 61\,\mu$m (see Fig. 6). In this experiment only, the TI turbulent regime is found, so the values of α_2 and γ_{TII} cannot be estimated from the experiments. According to our results, γ_{TI} is still that for wide channels, whereas for α_1 the value $\alpha_1 = -1$ has to be taken. From the expression (3.9), we find $Re_1 = 12$ (which confirms the first transition) and $Re_2 = 99$. For the coefficient γ_{TII}, we have chosen the same value used in Fig. 5, while for α_2 a tentative value is taken ($\alpha_2 = -2$). The difference $V_{\text{edge}} - V_{c2}$ is still the same that for wide channel.

In Figs. 7 and 8, the corresponding numerical results found in our model have been plotted for $d = 50\,\mu$m. There, we have used the value γ_{TI} of the wide channel, and a value slightly higher for γ_{TII}. The values of α_1 and α_2 are the same used for the channel of diameter $d = 61\,\mu$m. The Reynolds

numbers are again calculated according to formula (3.9), obtaining $Re_1 = 11$ and $Re_2 = 93$. The difference $V_{\text{edge}} - V_{c2}$ is the same that for wide channel. Heat transfer in He II in tubes of this order of size has been explored experimentally in [15]. As already pointed out, this choice of α_1 agrees with the prediction that α_1 is a slowly increasing function of the diameter of the channel.

These estimations as well as the graphics plotted in Fig. 4 show that the higher is the heat current the higher is the radius corresponding to the transition between all these regimes. Furthermore, the effective thermal conductivity drops down in the TI turbulent regime and much more in the TII regime. Thus, in order to cool down the temperature of a device, it is convenient to choose channels which show an effective thermal conductivity closer to the Landau's estimations. For a fixed heat current, this means that the radius of the channels has to be large enough in order to be in $L = 0$ regime or in the TI regime. Another observation is that these features depend on the temperature, and graphics show that lower temperature are preferable.

4. Conclusions

In Sect. 3 of this paper, we have established theoretically a more complete relation between ΔT and $\dot{Q}$, and the corresponding effective thermal conductivity of microchannels filled with He II in absence of net mass convection (counterflow situation). To do that, we have taken into consideration the resistance force due to quantized vortex tangle arising for high enough heat flux and, instead of assuming that $L \sim q^2$, as it follows from Vinen's equation (3.1), we have taken more detailed approach. This is based on Eq. (3.3), generalizing (3.1) through a term related to the influence of the walls on the vortex lines. This equation, and the behavior (3.7), (3.8) for their coefficients, yields an explicit mathematical model for the effective thermal conductivity of He II between Landau and Gorter–Mellink regimes. Unfortunately, this is not a simple expression, but it allows to bridge the gap between the two mentioned well-known regimes by means of an explicit physical model.

Since our aim was also to describe the full transition from laminar to fully turbulent regime by proposing the evolution equation (3.3) for L, it is worth to recall an analogous attempt carried out by Childers and Tough in 1976 [23]. Their aim was restricted to describe the transition from laminar regime to TI regime, with attention to the existence of two branches for L as function of $\dot{Q}$, the upper one being the usually observed one, and the lower one being metastable. Childers and Tough [23] wrote for the evolution equation for L

$$\frac{\mathrm{d}L}{\mathrm{d}t} = AL^{3/2} v_{ns} \left[1 - \frac{\alpha}{L^{1/2} d}\right] - \beta_v \kappa L^2 \tag{4.1}$$

where $A = \frac{1}{2}\chi_1 B \frac{\rho_n}{\rho}$. Equation (4.1) is similar to our equation (3.3), except for the second term having the form $L v_{ns} d^{-1}$ instead of our third term proportional to $L^{3/2}\kappa d^{-1}$. Both terms have the same dimensions and have the diameter d of the channel at the denominator in order to take into account the presence of the walls. Childers and Tough's proposal describes well the transition from laminar to TI regime, and the metastable solution of L, which is not described by our model, but it does not describe the TII turbulence. In contrast, our model describes the transition among the three states (laminar, turbulent TI and TII). This is so, in fact, because of the dependence (3.7) and (3.8) of the coefficient $\gamma_0(Re)$ and $\omega'(Re)$ on the quantum Reynolds number, which is necessary to go from the smaller slope of the line corresponding to TI turbulence to the steeper slope of the line corresponding to fully developed TII turbulence. For more exhaustive studies on the metastable solution between laminar and turbulent regimes, we also address the reader to the review [34].

This method cannot be extended to arbitrary narrow channels, because when the width of the channels becomes comparable or smaller than the mean free path of the heat carriers, the regime becomes ballistic and phonon collisions with the walls, rather than with rotons or with themselves, become the dominant factor [5,6,14,44]. Another aspect limiting the flow of heat from solid walls to liquid helium is the Kapitza conductance of the interface [45], but we do not deal with this topic here.

Note that, we have used as a relevant parameter in our description the Reynolds quantum number $v_{ns}d/\kappa$ instead of the classical Reynolds number $v_n d/\nu$. This is a difference with Arp's analysis, which assumed that turbulence TII corresponds to the setting of turbulence in the normal component, instead of assuming a sudden increase of vortex length density as the consequence of vortex line reconnection.

From a practical perspective, our paper indicates that, for a given amount of helium, better contact is achieved between a solid and the bulk He II if the contact is made through a few wider channels rather than many narrow channels. This is already known and experimentally confirmed [1,7]. For instance, for a certain given heat flux density, a large channel or ten small channels are used, all of them in laminar regime, the temperature difference is larger in the large channel (proportional to the square of the radius). However, this is no longer so in the turbulent regime. Thus, an understanding of the transition regime may be especially useful in cooling systems with high heat loads.

This may be useful for practical purposes. In particular, the present analysis shows the interest of Eq. (3.3) generalizing the usual Vinen's equation to take into account the effects of the walls. Such equation describes in a natural way the transition from laminar to turbulent TI state and, if it is complemented with (3.7) and (3.8), it also describes the transition from TI to TII turbulence. As it has been shown here, Eq. (3.3) is deeply related to the more practical topic of the effective thermal conductivity of narrow tubes filled with He II [1].

Acknowledgments

The authors acknowledge the support of the Università di Palermo (under Grant Nos. Fondi 60 % 2012 and Progetto CoRI 2012, Azione d) and the collaboration agreement between Università di Palermo and Universitat Autònoma de Barcelona. DJ acknowledges the financial support from the Dirección General de Investigación of the Spanish Ministry of Economy and Competitiveness under Grant FIS2012-32099 and of the Direcció General de Recerca of the Generalitat of Catalonia, under grant 2009 SGR-00164. M.S. acknowledges the hospitality of the "Group of Fisica Estadistica of the Universitat Autònoma de Barcelona". M.S. acknowledges the financial support of "National Group of Mathematical Physics" GNFM-INdAM and Progetto CORI 2011, Azione d.

References

1. Van Sciver, S.W.: Helium Cryogenics, 2nd edn. Springer, Berlin (2012)
2. Jones, M.C., Arp, V.D.: Review of hydrodynamics and heat transfer for large helium cooling systems. Cryogenics **18**, 483–490 (1978)
3. http://www.esa.int/TEC/Thermal_control/SEMZOWBE8YE_0.html
4. Bruus, H.: Theoretical Microfluidics. Oxford University Press, Oxford (2007)
5. Tabeling, P.: Introduction to Microfluidics. Oxford University Press, Oxford (2005)
6. Bertman, B., Kitchens, T.A.: Heat transport in superfluid filled capillaries. Cryogenics **8**, 36–41 (1968)
7. Arp, V.: Heat transport through helium II. Cryogenics **10**, 96–106 (1970)
8. Brewer, D.F., Edwards, D.O.: The Heat Conductivity and Viscosity of Liquid Helium II. Proc. R. Soc. Lond. A **251**, 247–264 (1959)
9. Brewer, D.F., Edwards, D.O.: Heat conduction by liquid helium II in capilliary tubes. I: Transition to supercritical conduction. Philos. Mag. **6**(66), 775–790 (1961)
10. Brewer, D.F., Edwards, D.O.: Heat conduction by liquid helium ii in capillary tubes II. Measurements of the pressure gradient. Philos. Mag. **6**, 1173–1181 (1961)
11. Brewer, D.F., Edwards, D.O.: Heat conduction by liquid helium II in capillary tubes III. Mutual friction. Philos. Mag. **7**, 721–735 (1962)
12. Kimura, N., Nakai, H., Murakami, M., Yamamoto, A., Shintomi, T.: A study on the heat transfer properties of pressurized Helium II through fine channels. AIP Conf. Proc. **823**, 97–104 (2006)
13. Chase, C.E.: Thermal Conduction in Liquid Helium II. I. Temperature dependence. Phys. Rev. **127**, 361–370 (1962)

14. Schmidt, R., Wiechert, H.: Heat transport of helium II in restricted geometries. Zeitschrift Fur Physik B Condensed Matter **36**, 1–12 (1979)
15. Granieri, P.P., Baudouy, B., Four, A., Lentijo, F., Mapelli, A., Petagna, P., Tommasini, D.: Steady-state heat transfer through micro-channels in pressurized He II. AIP Conf. Proc. **1434**, 231–238 (2011)
16. Landau, L.D., Lifshitz, E.M.: Fluid Mechanics. Elsevier, Oxford (1987)
17. Vinen, W.F.: Mutual friction in a heat current in liquid helium II. III. Theory of the mutual friction. Proc. R. Lond. A **240**, 493–515 (1957)
18. Donnelly, R.J.: Quantized Vortices in Helium II. Cambridge University Press, Cambridge (1991)
19. Barenghi, C.F., Donnelly, R.J., Vinen, W.F.: Quantized Vortex Dynamics and Superfluid Turbulence. Springer, Berlin (2001)
20. Nemirovskii, S.K.: Quantum turbulence: theoretical and numerical problems. Phys. Rep. **524**, 85–202 (2013)
21. Tsubota, M., Kobayashi, M., Takeuchi, H.: Quantum hydrodynamics. Phys. Rep. **522**, 191 (2011)
22. Martin, K.P., Tough, J.T.: Evolution of superfluid turbulence in thermal counterflow. Phys. Rev. B **27**, 2788–2799 (1983)
23. Childers, R.K., Tough, J.T.: Helium II thermal counterflow: temperature- and pressure-difference data and analysis in terms of the Vinen theory. Phys. Rev. B **13**, 1040–1055 (1976)
24. Keesom, W.H., Keesom, D.P., Saris, B.F.: A few measurements on the heat conductivity of liquid helium II. Physica **5**, 281–285 (1938)
25. Keesom, W.H., Saris, B.F., Meyer, L.: New measurements on the heat conductivity of liquid helium II. Physica **7**, 817–830 (1940)
26. Keesom, W.H., Duyckaerts, G.: Mesures sur la conductibilité thermique et l'effet thermomécanique de l'helium liquide II. Physica **13**, 153–179 (1947)
27. Allen, J.F., Ganz, E.: The influence of pressure on the thermal conductivity of liquid He II. Proc. R. Soc. A **171**, 242–250 (1939)
28. Allen, J.F., Reekie, J.: Momentum transfer and heat flow in liquid helium II. Proc. Camb. Philos. Soc. **35**, 114–122 (1939)
29. Winkel, P., Delsing, A.M.G., Poll, J.D.: On the existence of critical velocities in liquid helium II. Physica **21**, 331–344 (1955)
30. Fairbank, H.A., Wilks, J.: Heat Transfer in Liquid Helium below 1 degrees K. Proc. R. Soc. A **231**, 545–555 (1955)
31. Mendelsohn, K.: Liquid Helium, Encyclopedia of Physics, vol. XV. Springer, Berlin (1956)
32. Jou, D., Sciacca, M.: Quantum Reynolds number for superfluid counterflow turbulence. Boll. di mat. Pura ed appl.VI (2014), 95–103, ISBN: 978-88-548-6942-4
33. Mongiovì, M.S.: Extended irreversible thermodynamics of liquid helium II. Phys. Rev. B **48**, 6276–6283 (1993)
34. Mongiovì, M.S., Jou, D.: Evolution equations in superfluid turbulence. In: Das, M.P. Condensed Matter: New Research, pp. 1 Nova Science Publishers, New York (2007)
35. Tisza, L.: Transport phenomena in helium II. Nature **141**, 913 (1938)
36. Jou, D., Casas-Vázquez, J., Criado-Sancho, M.: Thermodynamics of Fluids Under Flow, 2nd edn. Springer, Berlin (2011)
37. Mongiovì, M.S.: Extended irreversible thermodynamics of liquid helium II: boundary condition and propagation of fourth sound. Physica A **292**, 55–74 (2001)
38. Mongiovì, M.S., Jou, D.: Generalization of Vinen's equation including transition to superfluid turbulence. J Phys. Condens. Matter **17**, 4423–4440 (2005)
39. Sooraj, R., Sameen, A.: Effect of vortex line distribution in superfluid plane Poiseuille flow instability. J. Fluid Mech. **720**, R1–15 (2013)
40. Galantucci, L., Barenghi, C.F., Sciacca, M., Quadrio, M., Luchini, P.: Turbulent Superfluid Profiles in a Counterflow Channel. J. Low Temp. Phys. **162**, 354–360 (2011)
41. Donnelly, R.J., Barenghi, C.F.: The observed properties of liquid helium at the saturated vapor pressure. J. Phys. Chem. Ref. Data **27**, 1217–1274 (1998)
42. Melotte, D.J., Barenghi, C.F.: Transition to normal fluid turbulence in helium II. Phys. Rev. Lett. **80**, 4181–4184 (1998)
43. Brugarino, T., Mongiovì, M.S., Sciacca, M.: Waves on a vortex filament: exact solutions of dynamical equations. Z. Angew. Math. Phys. (2014)
44. Sciacca, M., Sellitto, A., Jou, D.: Transition to ballistic regime for heat transport in helium II. Phys. Lett. A **378**, 2471–2477 (2014)
45. Snyder, N.S.: Heat transport through helium II: Kapitza conductance. Cryogenics **10**, 89–95 (1970)

M. Sciacca
Dipartimento di Scienze Agrarie e Forestali
Università di Palermo
Viale delle Scienze
90128 Palermo
Italy
e-mail: michele.sciacca@unipa.it

M. Sciacca and D. Jou
Departament de Física
Universitat Autònoma de Barcelona
08193 Bellaterra
Catalonia
Spain

D. Jou
Institut d'Estudis Catalans
Carme 47
08001 Barcelona
Catalonia
Spain
e-mail: david.jou@uab.cat

M. S. Mongiovì
Dipartimento di Ingegneria Chimica, Gestionale, Informatica, Meccanica
Università di Palermo,
Viale delle Scienze
90128 Palermo
Italy
e-mail: m.stella.mongiovi@unipa.it

(Received: November 28, 2013; revised: September 16, 2014)